

# Effects of Vapothermal Pretreatment on Anaerobic Degradability of Common Reed

Marvin Scherzinger,\* Martin Kaltschmitt, and Mario Thoma

Residual materials from currently unused plant matter are available locally in abundance and serve as a valuable substrate for biogas production via anaerobic digestion. However, in most cases, a pretreatment is necessary to overcome their recalcitrant behavior. Against this background, earlier ground biomass from *Phragmites australis*, better known as common reed, is pretreated in a vapothermal atmosphere at temperatures between 122 and 178 °C and residence times between 18 and 102 min. Herein, the influence of such a pretreatment on the specific biogas and methane yield is aimed to be evaluated. In addition, the main causes for changes in degradability are identified by means of accompanying analytics. It is found that vapothermal pretreatment is able to significantly enhance degradation velocity during anaerobic digestion. However, under severe conditions, the biogas and methane yields decrease, which is traced back to an increase in cellulose crystallinity, inaccessibility of pores due to precipitated reaction products, as well as the formation of inhibiting substances and proportional increase in nondegradable lignin.

## 1. Introduction

Biogas, which consists of the two main components methane (CH<sub>4</sub>) and carbon dioxide (CO<sub>2</sub>), has been used as an energy source for quite some time. In industrial nations such as Germany, there have been three phases to date in which the technical production of biogas has experienced an upswing. The first technical biogas plants built in the 1950s were shut down after a short period of operation due to decreasing oil prices. During the 1973 oil crisis, biogas was increasingly used again for energy provision, but due to the subsequent sharp drop in crude oil prices,

the technology was not further developed. The third upswing period began in the early 1990s and can be linked to changed framework conditions in the waste and recycling industry. Due to the politically forced expansion of renewable energy, Germany has seen the strongest increase in biogas plants in the world to date.<sup>[1]</sup> However, this increase is currently slowing down as a result of political changes in monetary compensation.<sup>[2]</sup> Despite the decelerated growth in the construction of new plants, the potential of energetic biogas use is far from being exhausted. However, undesired side effects of agricultural energy crop production and lack of public participation led to a poor image of biogas plants in large parts of the population in the past years.<sup>[3]</sup> This could at least partly be counteracted by increasingly using residual materials for biogas production, as there is no competition for land use and no emissions associated with cultivation. Among others, reed grass is such a waste substrate with relatively high potential due to its strong distribution together with high crop yields.<sup>[4]</sup> For example, *Phragmites australis*, one of the most widely distributed wetland plant species worldwide, has an above-ground potential ranging from around 3 to 30 t ha<sup>-1</sup> a<sup>-1</sup>. The global harvestable above-ground biomass from reeds is estimated at 10 million t a<sup>-1</sup>.<sup>[5]</sup> However, biogas production from reed is currently not widespread due to various constraints. In most regions, the harvest is usually done in winter. This minimizes conflict with nature conservation (e.g., breeding birds) and is easier and cheaper when the ground is frozen and therefore accessible for agricultural machinery. However, reed straw harvested in winter contains fewer nutrients as their largest share is transported to the rhizomes at that time. Furthermore, the above-ground biomass is more lignified at that time,<sup>[6]</sup> which reduces the anaerobic degradability. Moreover, the translocation of nutrients to the rhizomes leads also to lower content of inorganics, making this organic material rather suitable as a solid combustible due to reduced ashing problems. Low nutrient contents can be compensated in anaerobic fermentation, e.g., by cofermentation with more nutrient-rich substrates. To allow anaerobic fermentation of lignin-rich biomass under commercial conditions, a pretreatment in which the recalcitrant material is broken down is necessary. Several technologies are currently available to achieve this goal. These can be assigned to different groups, e.g., there are biological, physical, chemical, and thermal processes. One specific advantage of thermal processes is that

M. Scherzinger, Prof. M. Kaltschmitt  
Hamburg University of Technology (TUHH)  
Institute of Environmental Technology and Energy Economics (IUE)  
Eissendorfer Strasse 40, 21073 Hamburg, Germany  
E-mail: marvin.scherzinger@tuhh.de

M. Thoma  
Bauer Resources GmbH  
Bauer-Strasse 1, 86529 Schrobenhausen, Germany

 The ORCID identification number(s) for the author(s) of this article can be found under <https://doi.org/10.1002/ente.202001046>.

© 2021 The Authors. Energy Technology published by Wiley-VCH GmbH. This is an open access article under the terms of the Creative Commons Attribution-NonCommercial-NoDerivs License, which permits use and distribution in any medium, provided the original work is properly cited, the use is non-commercial and no modifications or adaptations are made.

DOI: 10.1002/ente.202001046

they can be implemented at relatively low cost when there is excess heat available. This is usually the case as most biogas plants convert biogas into electricity on site in a combined heat and power plant. In this context, the present article aims to investigate the effects of vapothermal pretreatment on the anaerobic digestibility of above-ground reed biomass. Special attention is paid to the effects of temperature and residence time. To explain the observed effects during anaerobic digestion, different properties of the treated biomass are also investigated.

## 2. Experimental Section

### 2.1. Material

Above-ground reed biomass (*Phragmites australis*) was sampled from a constructed wetland in the sultanate of Oman in June 2019. The upper part of the stalks, which did not come in contact with the wastewater to be treated in the constructed wetland, was used for this study. To preserve the sampled biomass, it was air dried in the sun to a water content of  $6.0 \pm 0.1$  wt.% and precut to pieces with a length of about 10 cm.

### 2.2. Vapothermal Pretreatment

Vapothermal pretreatment was conducted in a technical-scale rotation reactor ( $V = 65$  L) equipped with electric wall heating (custom-built, Estanit, Germany). In principle, this pretreatment is equal to a rotating steam autoclaving. In the first step, the reed was precut with garden shears to a maximum length of 10 cm, and a total of  $200 \pm 1$  g was placed into a cylindrical revolving spit basket made of stainless steel (diameter = 13.8 cm; length = 32.0 cm; volume = 4.8 L; and mesh size = 4 mm) in each experimental run. The basket was then screwed onto a stainless steel rod in the middle of the reactor, so that it could be continuously rotated during pretreatment. In addition, 2 L tap water was filled into the reactor before it was closed. The revolving spit basket did not come into contact with the water (see **Figure 1**). After closing the reactor, it was heated until a saturation pressure in accordance with the desired treatment temperature was reached (2.1 bar at 122 °C, 2.7 bar at 130 °C, 4.8 bar at 150 °C, 7.9 bar at 170 °C, and 9.5 bar at 178 °C). The heating rate was  $10\text{ °C min}^{-1}$  and the rotational speed was  $5\text{ min}^{-1}$ . After reaching the treatment temperature, the residence time started and the

temperature was kept constant at the desired level. After expiration of the residence time, the pressure was reduced to ambient conditions within 3 min maximum by opening a valve, and the reed samples pretreated in this way were removed for further investigations.

### 2.3. Experimental Design and Statistical Analysis

The experiments were planned according to a rotatable central composite design (CCD), as shown in **Table 1**. This design allows both efficient estimation of first- and second-order terms.<sup>[7]</sup> It consists of a two-stage experimental design, which is extended by four further test runs starting from the center point. The center point was tested five times to estimate pure error. Hence, a total of 13 experimental runs were conducted in random order; the respective conditions of the tests with regard to the variation of the factors are shown in **Table 2**. The experimental data were analyzed using the statistical software DesignExpert Version 9.0.5.1 (Stat-Ease Inc., Minneapolis, USA) as well as SPSS Statistics 24 (IBM, New York, USA). A variance analysis was conducted for each of the different parameters examined. To determine statistically significant differences, the Tukey–Kramer posthoc test, which is especially suitable for unequal group sizes, was conducted at a significance level of  $\alpha = 0.05$ .<sup>[8]</sup>

### 2.4. Determination of Characteristic Values

With the exception of the determination of moisture content, all samples were dried in a static standard drying oven (U80, Memmert, Germany) at 105 °C over night and ground in a knife mill (MF10, IKA, Germany) equipped with a sieve (mesh width = 3 mm) before conducting the analyses described below.

**Table 1.** Process factors, range, and levels in experimental design.

Factors	Symbols	Coded levels				
		$-\sqrt{2}$	-1	0	1	$\sqrt{2}$
Temperature [°C]	A	122	130	150	170	178
Residence time [min]	B	18	30	60	90	102

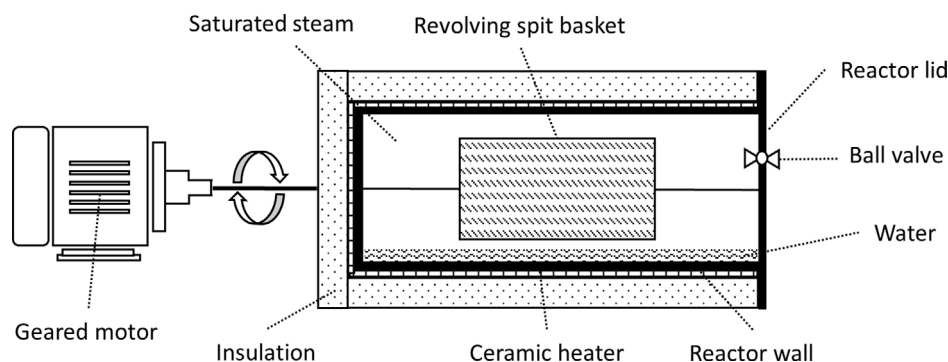


**Figure 1.** Simplified representation of the reactor used for vapothermal pretreatment.

**Table 2.** Characteristic values of the investigated reed biomass before and after vapothermal pretreatment—different letters indicate significant differences between mean values according to the Tukey–Kramer test ( $\alpha = 0.05$ ).

Sample	X	VS	HHV	pH	WHC	Hemicellulose	Cellulose	Lignin	Others
Untreated	0.07 <sup>A</sup>	94.7 <sup>BCDE</sup>	18.3 <sup>ADFG</sup>	4.89 <sup>A</sup>	7.2 <sup>A</sup>	22.7 <sup>A</sup>	48.0 <sup>A</sup>	12.5 <sup>A</sup>	16.8 <sup>A</sup>
122 °C 60 min	0.15 <sup>DF</sup>	95.2 <sup>E</sup>	18.5 <sup>BCEF</sup>	4.24 <sup>C</sup>	7.2 <sup>A</sup>	20.3 <sup>B</sup>	48.9 <sup>A</sup>	16.3 <sup>AB</sup>	14.5 <sup>A</sup>
130 °C 30 min	0.13 <sup>CEF</sup>	95.2 <sup>E</sup>	17.7 <sup>A</sup>	4.42 <sup>B</sup>	7.9 <sup>AB</sup>	20.8 <sup>AB</sup>	48.6 <sup>A</sup>	14.6 <sup>AB</sup>	16.0 <sup>A</sup>
130 °C 90 min	0.14 <sup>DF</sup>	94.3 <sup>AE</sup>	18.0 <sup>AB</sup>	4.12 <sup>CD</sup>	7.9 <sup>AB</sup>	20.0 <sup>B</sup>	50.1 <sup>A</sup>	14.8 <sup>AB</sup>	15.1 <sup>A</sup>
150 °C 18 min	0.13 <sup>CDF</sup>	94.2 <sup>AD</sup>	18.1 <sup>AC</sup>	4.05 <sup>D</sup>	7.9 <sup>AB</sup>	19.1 <sup>B</sup>	50.6 <sup>A</sup>	13.6 <sup>AB</sup>	16.7 <sup>A</sup>
150 °C 60 min	0.12 <sup>BC</sup>	94.8 <sup>CDE</sup>	18.3 <sup>BCD</sup>	3.52 <sup>E</sup>	8.5 <sup>B</sup>	9.7 <sup>C</sup>	48.5 <sup>A</sup>	15.3 <sup>AB</sup>	26.5 <sup>B</sup>
150 °C 102 min	0.12 <sup>BDE</sup>	94.0 <sup>AC</sup>	18.3 <sup>ADE</sup>	3.29 <sup>H</sup>	8.1 <sup>AB</sup>	5.0 <sup>D</sup>	48.1 <sup>A</sup>	18.3 <sup>BC</sup>	28.5 <sup>B</sup>
170 °C 30 min	0.10 <sup>AB</sup>	93.6 <sup>A</sup>	18.6 <sup>CEG</sup>	3.49 <sup>EF</sup>	7.8 <sup>AB</sup>	4.3 <sup>D</sup>	46.2 <sup>A</sup>	19.0 <sup>BC</sup>	30.5 <sup>B</sup>
170 °C 90 min	0.08 <sup>A</sup>	93.8 <sup>AB</sup>	18.8 <sup>EG</sup>	3.40 <sup>F<sup>GH</sup></sup>	4.4 <sup>C</sup>	2.7 <sup>D</sup>	47.0 <sup>A</sup>	23.4 <sup>CD</sup>	26.8 <sup>B</sup>
178 °C 60 min	0.15 <sup>F</sup>	94.4 <sup>AE</sup>	19.4 <sup>H</sup>	3.43 <sup>EG</sup>	4.7 <sup>C</sup>	2.8 <sup>D</sup>	47.7 <sup>A</sup>	25.1 <sup>D</sup>	24.4 <sup>B</sup>
Pooled standard error	±0.01	±0.2	±0.1	±0.02	±0.4	±0.5	±0.4	±0.5	±0.5

#### 2.4.1. Moisture Content, Volatile Solids, Higher Heating Value, and pH Value

Moisture content ( $X$ ) was measured 1 h after vapothermal pretreatment. In the meantime, reed samples were exposed to ambient conditions. For determination,  $20 \pm 1$  g were weighed into aluminum bowls ( $V = 0.6$  L) and dried at  $105^\circ\text{C}$  overnight.  $X$  was then calculated according to Equation (1). Volatile solids (VSs) of both untreated and treated reed samples were determined according to DIN EN 15935<sup>[9]</sup> in triplicates. For this purpose,  $1.0 \pm 0.1$  g of dry sample each was put into melting crucibles made of glazed porcelain and incinerated at  $550^\circ\text{C}$  in a muffle furnace (M 104, Thermo Scientific Heraeus, USA). Contents of VSs were subsequently calculated according to Equation (2).

$$X = \frac{m_w - m_d}{m_d} \quad (1)$$

$m_w$  is the total mass of wet sample after 1 h and  $m_d$  is the mass after drying. In the following, the results of  $X$  are therefore given as mass of water per mass of dry matter [g<sub>w</sub> g<sub>DM</sub><sup>-1</sup>]:

$$w_{VS} = \frac{m_b - m_c}{m_b - m_a} \times 100 \quad (2)$$

$w_{VS}$  is the amount of VS based on dry matter.  $m_a$  is the mass of the empty crucible,  $m_b$  is the mass of the crucible after addition of dry sample mass, and  $m_c$  is the mass of the crucible and ash remainder after incineration.

Higher heating value (HHV) was analyzed in duplicates according to DIN 51900 using a bomb calorimeter (C200, IKA, Germany).

pH value was measured according to DIN EN 15933 after creating a suspension of reed sample ( $1 \pm 0.1$  g) and 20 mL demineralized water.<sup>[10]</sup>

#### 2.4.2. Cell Wall Components

Cell wall components (i.e., hemicellulose, cellulose, and lignin) were determined according to the method book of the Association of German Agricultural Research Institutes, Volume III.<sup>[11]</sup> This method consisted of three consecutive treatment steps followed by incineration of the remainder. Summarizing, the method is described as follows. 1) A beaker was filled with 360 mL neutral detergent solution (ND solution) and heated to boiling point; then, 2 mL heat-stable  $\alpha$ -amylase (Termamyl 120 L, Type L, Novozymes) was added. About 1 L of the ND solution consisted of distilled water, in which 30.0 g of dodecyl sulfate sodium salt, 18.61 g of ethylenediamine-tetraacetic acid disodium dehydrate, 6.81 g of sodium borate decahydrate, 4.56 g of disodium hydrogen phosphate, and 10.0 mL of triethyleneglycol were dissolved. The pH value of the solution was adjusted to 7.0 by adding acetic acid before its use. A sample carousel containing six fiber bags with  $1 \pm 0.1$  g dry sample mass and each was put in the beaker for 1 h. Then, the fiber bags were extracted and rinsed with distilled water. The remaining residue after drying at  $105^\circ\text{C}$  over night was the neutral detergent fiber, containing hemicellulose, cellulose, lignin, and inorganics. 2) The procedure was repeated using 360 mL of an acid solution consisting of sulfuric acid ( $c = 0.5 \text{ mol L}^{-1}$ ) and 20 g hexadecyltrimethylammonium bromide  $\text{L}^{-1}$ . As starting material, the neutral detergent fiber was used. The remaining residue after rinsing with distilled water and drying at  $105^\circ\text{C}$  was the acid detergent fiber, containing cellulose, lignin, and inorganics. 3) The cellulose component within the acid detergent fiber was removed by submerging it in a 72% aqueous sulfuric acid solution for 3 h. Then, the remainder was washed until it was acid free and dried at  $105^\circ\text{C}$  over night. To be able to deduct the inorganic components from lignin content, the samples were incinerated at  $550^\circ\text{C}$ , according to the method described earlier for determination of VSs. 4) The difference between cell wall components measured in this way and the total mass of sample can be summarized as “others.”

### 2.4.3. Particle Size Distribution and Water-Holding Capacity

Particle size distribution was determined by sieve tower method according to DIN 51938 in duplicates.<sup>[12]</sup> Therefore,  $20 \pm 1$  g of each ground sample was placed on a sieve tower (Analysette 3, Fritsch, Germany) equipped with a series of sieves of mesh sizes 1000, 630, 355, 200, 125, and 63  $\mu\text{m}$ . After 5 min of sieving at an amplitude of 1.0, the mass on each sieve was measured and recorded as a percentage of the original sample mass.

Water-holding capacity (WHC) was determined by placing  $1.0 \pm 0.1$  g of each sample in a glass funnel lined with folding filter (pore size = 5  $\mu\text{m}$ ) in triplicates. About 50 mL of deionized water was added slowly until the sample was saturated and the water was allowed to drain by gravity for 3 h. The final moisture content was determined gravimetrically by drying method at 105 °C. The results were corrected for the moisture adsorbed by the folding filter and the results were again presented as mass of water per mass of dry matter [ $g_w g_{DM}^{-1}$ ].

### 2.4.4. Cellulose Crystallinity

Fourier-transform infrared (FTIR) spectrophotometer (Alpha T, Bruker, Germany) was used to determine the cellulose crystallinity index (CI). For this purpose, the samples were additionally further ground to a particle size of <1 mm using the same knife mill as described in Section 2.4. Subsequently, a KBr compact was produced using the macropress technique, as described in the study by Gunzler et al.<sup>[13]</sup> The used KBr (KBr for IR spectroscopy, Carl Roth, Germany) was dried at 150 °C and cooled down in a desiccator before its use. To avoid recrystallization during compact production, the applied force of  $10^5$  N was maintained for 2 min. Spectra were recorded as an average of 32 scans with a resolution of 2  $\text{cm}^{-1}$  in a range from 4000 to 400  $\text{cm}^{-1}$ . CI was calculated as proposed by Hurtubise and Krassig<sup>[14]</sup> and expanded by Nelson and O'Connor<sup>[15]</sup> as the ratio of absorbance peak heights at 1427 and 898  $\text{cm}^{-1}$ , whereby the former peak was assigned to a symmetric  $\text{CH}_2$  bending vibration (known as “crystallinity band”) and the latter was assigned to C–O–C stretching at  $\beta$ -(1,4)-glycosidic linkages (known as “amorphous band”).<sup>[16]</sup>

## 2.5. Biogas Formation and Kinetics

Biogas yields were determined according to the VDI guideline 4630<sup>[17]</sup> under mesophilic conditions at  $37 \pm 1$  °C in batch tests. About 500 mL glass bottles were used as reactors and the investigation was conducted in triplicates for each experimental run. In a first step, the glass bottles were filled with  $400 \pm 1$  g of digested sludge, which was obtained from a municipal sewage treatment plant located a few kilometers south of Hamburg, Germany. This inoculum was allowed to outgas for 6 d. Then, 2.7  $g_{VS}$  of ground reed samples (grinding was conducted in the same way as described in Section 2.4) was placed in each reactor. A reference measurement was carried out in three reactors without addition of the substrate. To check the biological activity of the digested sludge used, three reactors were also fed with microcrystalline cellulose powder (A17730, Alfa Aesar, USA). Each trial was conducted for 32 days from substrate

addition during which the samples were manually stirred once a day. The amount of biogas formed during this time was measured by the use of eudiometer tubes connected to the sample bottles and filled with a sealing liquid consisting of a sodium chloride solution acidified with citric acid. The methane content of the gas formed was measured using a portable gas analyzer (Biogas 5000, Geotech, Italy) equipped with a dual-wavelength IR sensor.

The averaged data of biogas production were further used in kinetic model fitting. More precisely, nonlinear kinetic model fitting was conducted using “Jupyter Notebook Version 6.1.4.” Two different types of models were developed for the series of measurements carried out, one based on a modified Gompertz equation (Equation (3)) and the other based on a transference equation (Equation (4)). With both types of models, the maximum biogas production potential ( $P$  in  $\text{mL}_N g_{VS}^{-1}$ ), maximum rate of biogas production ( $R_m$  in  $\text{mL}_N g_{VS}^{-1} d^{-1}$ ), and duration of lag phase ( $\lambda$  in d) were determined.<sup>[18]</sup>

$$M = P \cdot \exp \left\{ -\exp \left[ \frac{R_m \cdot e}{P} (\lambda - t) + 1 \right] \right\} \quad (3)$$

$$M = P \left\{ 1 - \exp \left[ -\frac{R_m (t - \lambda)}{P} \right] \right\} \quad (4)$$

In the equations,  $M$  is the biogas yield in  $\text{mL}_N g_{VS}^{-1}$  with respect to time  $t$  in days and  $e$  is Euler’s constant. To check how well the models fit to the measured data, both the coefficient of determination ( $R^2$ ) and the root mean square error (RMSE) were calculated.

## 3. Results and Discussion

### 3.1. Effect of Vapothermal Pretreatment on Characteristic Values

Table 2 shows an overview of the characteristic values before and after vapothermal pretreatment. As explained in Section 2.3, the center point was tested five times to estimate pure error; in the table, these results are summarized in one column as mean value of all. This also applies to all other tables and figures, unless otherwise described. The results show that vapothermal pretreatment is able to significantly change both physical and chemical properties of reed biomass. A detailed consideration of the changes as a function of treatment temperature and residence time is given.

#### 3.1.1. Moisture Content, Volatile Solids, HHV, and pH

Table 2 shows the moisture content ( $X$ ) as well as the share of VSs and HHV for all samples.  $X$  increases with different strengths for all samples after treatment from 0.07 for untreated reeds up to 0.15  $g_w g_{DM}^{-1}$  after treatment at 122 °C and 60 min. This can be traced back to steam penetration during treatment. Water thereby still remains in the pores and adheres to the surface after treatment. However,  $X$  was still relatively low, especially when compared with other similar treatments like steam explosion, for which the treatment of reeds at 160 °C for 15 min led to  $X$  of 1.07  $g_w g_{DM}^{-1}$ .<sup>[19]</sup> This offers advantages when

transportation is required afterward, as it results in a greater proportion of organic substance per unit mass. In addition, there could also be benefits during subsequent storage of pretreated material as the material must then be dried again to prevent biodegradation, due to fungi growth, which can start at moisture contents of around  $0.12 \text{ g}_w \text{ g}_{DM}^{-1}$ .<sup>[20]</sup> However, further investigations should clarify whether, e.g., hornification of cellulose fibers limiting the use of pretreated reeds occurs, before subsequent storage is considered.<sup>[21]</sup>

It was noted that pH value decreases with increasing temperature and residence time. One explanation for this could be that during thermal pretreatment, the individual macromolecules are broken down into smaller molecules. This could cause the release of acetyl groups, esterified in hemicelluloses, as acetic acid. Furthermore, e.g., sugars could be hydrolyzed from hemicellulose, which can then further be degraded to acetic acid, leading to reduced pH values. For a more detailed consideration of the decomposition pathways of lignocellulosic material, refer to the study by Scherzinger et al.<sup>[22]</sup> The acids formed during vapothermal pretreatment can partially escape with the steam phase at the end of pretreatment, leading to reduced VS contents. However, for VS, only slight differences after vapothermal pretreatment were found. As mainly organic compounds are expelled, this indicates that the total mass loss is also low. For reeds pretreated via steam explosion at  $160^\circ\text{C}$ , mass losses of up to  $20\%_{DM}$  were mentioned.<sup>[19]</sup> Mass losses could be calculated using the ash content of both untreated and pretreated samples via Equation (5).<sup>[23]</sup>

$$\frac{\text{Mass loss}}{\text{Mass total}} = \frac{\text{Ash content}_{\text{pretreated sample}} - \text{Ash content}_{\text{untreated sample}}}{\text{Ash content}_{\text{untreated sample}}} \quad (5)$$

However, due to inhomogeneity of the reed material, a precise calculation of the mass loss in this way could not be carried out. However, it is expected that mass losses are in a similar range or even lower as earlier mentioned. This thesis was proven in further experiments for temperatures up to  $150^\circ\text{C}$  and residence times up to 80 min. Thereby, mass loss was determined by gravimetric detection of dry mass before and after vapothermal pretreatment, also using the example of reeds. The results showed that only a maximum of 3% mass loss occurred.

An indicator for comparatively low mass losses within the experiments presented here is, e.g., the HHV, which changes only slightly after vapothermal pretreatment at temperatures  $\leq 170^\circ\text{C}$ . Typically, an increase of HHV after vapor pretreatment can be traced back to a decrease in oxygen and hydrogen content by disintegration of the bonds within the biomass matrix. This is realized by the expulsion of easily hydrolysable components.<sup>[24]</sup> In contrast, this means that vapothermal pretreatment at temperatures  $\leq 170^\circ\text{C}$  did only separate relatively few plant components entirely. In general, it can be assumed that the less severe pretreatment conditions, the less the mass loss. This can be attributed to the thermal stability of the individual main components of reed. For instance, hemicellulose can be decomposed hydrolytically from  $\approx 150^\circ\text{C}$ , whereas lignin and cellulose start to decompose at around  $180^\circ\text{C}$  and over  $200^\circ\text{C}$  in a h

atmosphere, respectively.<sup>[25]</sup> Low mass losses are desirable as they are directly associated with energy losses.

### 3.1.2. Cell Wall Components

The total lignocellulosic fraction of untreated reed biomass (i.e., the sum of hemicellulose, cellulose, and lignin) was 82.7 wt.%. Cellulose made up the largest share in total, followed by hemicellulose. The third-largest share was made up of other components, which include cell ingredients such as pectins, starch, sugars, fats, and proteins, as well as inorganics. Lignin had the smallest share. The following results presented regarding the cell wall components refer to each respective sample used. Typically, these values are given related to the untreated biomass, which was not possible here due to the impossibility of determining the exact mass losses (see Section 3.1.1). However, as the mass losses are mostly estimated to be small, trends can still be identified.

At pretreatment temperatures below  $150^\circ\text{C}$ , the macromolecular composition hardly changed. This is in accordance with the information in the literature, according to which the cell wall components only decompose hydrolytically at temperatures  $\geq 150^\circ\text{C}$ .<sup>[25]</sup> However, starting at a treatment temperature of  $150^\circ\text{C}$ , significant decrease in hemicellulose content occurred. Thereby, longer residence times did also lead to higher decrease. This behavior is shown graphically in Figure 2. It must be mentioned that the response surface plot shown there serves for illustrative purposes only, as the underlying model overestimates the hemicellulose content at longer residence times at simultaneously lower temperatures. However, it becomes clear that at higher treatment temperatures, significantly shorter residence times are required for hemicellulose removal. The proportion of the cellulose fraction was comparatively slightly changed by vapothermal pretreatment.

The organic ingredients presented here can be degraded anaerobically to different degrees. Generally, when it comes to lignocellulosic biomass, the cell ingredients are the most easily degradable material, followed by hemicellulose and cellulose. Lignin cannot be degraded anaerobically.<sup>[26]</sup> Lignin content after vapothermal pretreatment was inversely proportional to

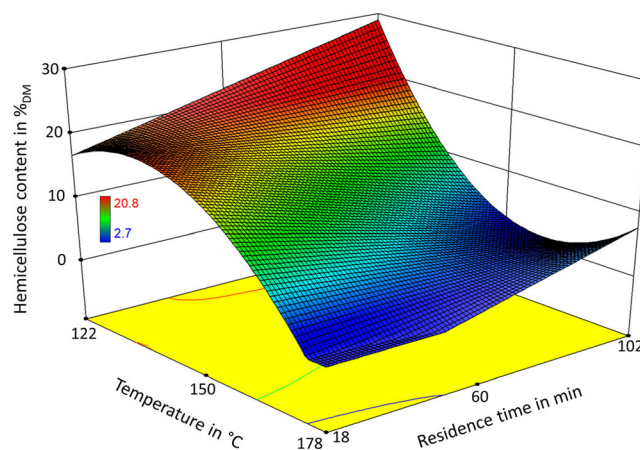


**Figure 2.** Response surface plot for hemicellulose content depending on temperature and residence time.

hemicellulose content, i.e., it increased with increasing temperature and residence time, starting at around 150 °C. This coincides with results from similar pretreatment methods like steam explosion and thermal pretreatment.<sup>[23,27]</sup> The increase in lignin content can have two different causes. 1) there is a loss of organic components like hemicellulose during vapothermal pretreatment, whereby the relative share of lignin increases, and 2) there are degradation products formed that are not soluble in acid and therefore measured as lignin during determination of cell wall components. Other positive effects may offset the negative effect of increased lignin content on anaerobic degradability, e.g., through the breakdown of hemicellulose, the accessibility of cellulose for microorganisms could be enhanced, leading to higher degradability.<sup>[27]</sup>

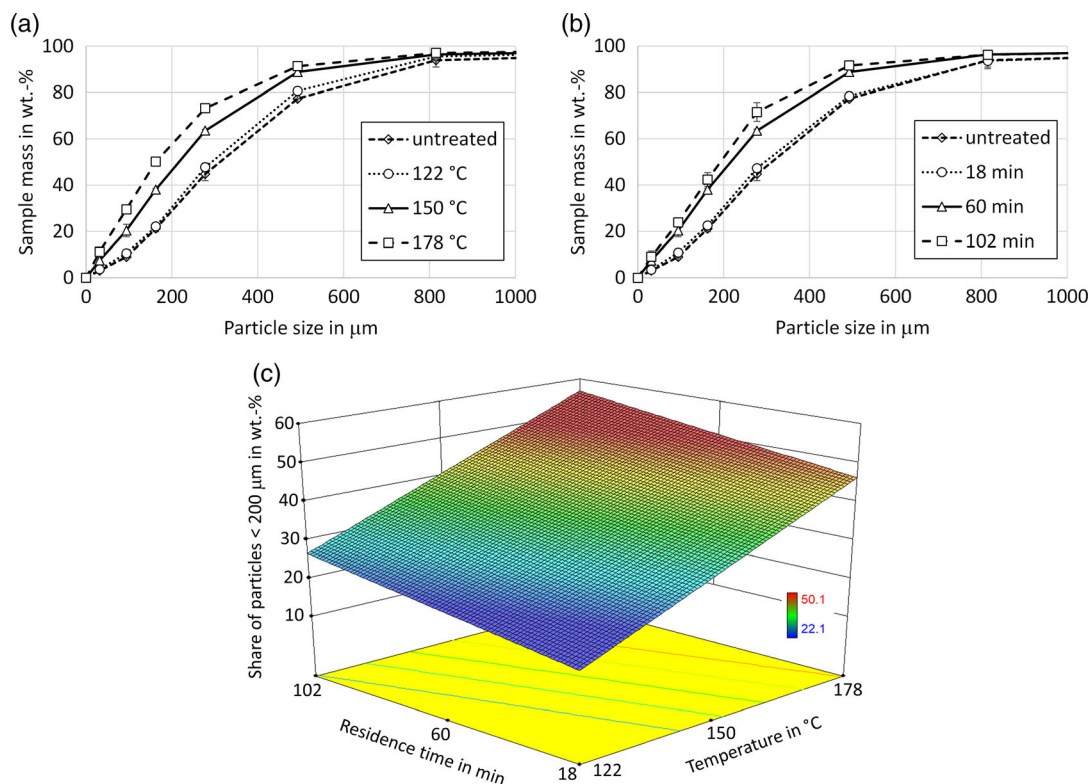
### 3.1.3. Particle Size Distribution and WHC

Figure 3a,b shows the particle size distribution of selected samples after comminution in a knife mill. It is well known that a grinding pretreatment often leads to significant higher anaerobic digestibility of lignocellulosic biomass. The main reasons therefore are both increase in the surface available for microorganisms and promotion of hydrolytic degradation.<sup>[28,29]</sup> From the displayed results, it becomes clear that vapothermal pretreatment can significantly influence particle size distribution after subsequent comminution. At temperatures < 150 °C, this influence is very slight, whereas at temperatures ≥ 150 °C, proportionately more particles with smaller sizes are present. At such high

temperatures, residence time leads to a higher proportion of particles with smaller diameters. This behavior is shown graphically in Figure 3c for particles < 200 μm. Again, the response surface plot serves only for illustrative purposes. In this case, the underlying model was not validated by further test measurements. However, it can be derived that the influence of temperature is higher compared with the influence of residence time. More particles with a smaller diameter are also an indicator of improved grindability. Most likely, improvement of grindability can be traced back to the aforementioned reduction of hemicellulose within the cell walls, which leads to a more hollow structure and weakens the structural framework. This was, e.g., proven for thermal pretreatment of lignocellulosic biomass in a gaseous atmosphere via torrefaction<sup>[30]</sup> and is also known for autoclave pretreatment of lignocellulosic biomass.<sup>[31]</sup> In addition, the vapothermal pretreatment may also have softened the lignin fraction, which might also be a reason for enhanced grindability.<sup>[32]</sup>

It is usually true that fibrous lignocellulosic biomass has to be comminuted to particle sizes of 1–2 mm to overcome heat and mass transfer limitations within hydrolysis, which is the first and often rate-limiting step during anaerobic digestion.<sup>[33]</sup> Such a reduction in particle size cannot be achieved by vapothermal pretreatment under the conditions investigated here. However, higher shares of small particles after comminution are an indirect proof of enhanced grindability.<sup>[34]</sup> The results therefore suggest that due to the pretreatment, the energy consumption during a subsequent comminution can be reduced.

While reduction in particle size primarily outlines changes in the external surface area, determination of the WHC aims to



**Figure 3.** a) Particle size distribution curves for untreated and vapo-thermally pretreated reed samples at a constant residence time of 60 min, b) at a constant treatment temperature of 150 °C, and c) response surface plot for particles < 200 μm depending on temperature and residence time.

enable conclusions about the porous structure within fiber walls. An increase in WHC thereby indicates enlargement in total pore volume, which also can lead to an increase in total surface area accessible for microorganisms during anaerobic digestion.<sup>[35]</sup> However, due to different reasons, this method can only serve to determine a trend and does not directly reflect the pore volume. On the one hand, water sorption is not limited only to pores but also can occur on the biomass surface.<sup>[36]</sup> On the other hand, cell components like lignin are hydrophobic by nature and therefore can lead to lower WHCs. Results of WHC measurements are shown in Table 2. For steam explosion pretreatment of safflower straw in a similar temperature range between 120 and 180 °C, an increase in WHC up to 124% was reported.<sup>[35]</sup> Vapothermal pretreatment conducted in this study at temperatures between 130 and 170 °C was also found to enable an increase in WHC. Largest increase of up to 26% was found for pretreatment at 150 °C for 60 min. On the contrary, significant decrease in WHC was found after vapothermal pretreatment at 170 °C for 90 min and at 178 °C for 60 min. This can either be traced back to a higher share of lignin or blocking of pores by precipitation of previously solubilized cell components. Summarizing, it can be stated that increase in WHC seems to be much weaker for vapothermal pretreatment compared with steam explosion. Furthermore, severe pretreatment conditions even lead to a decrease compared with the untreated sample, which might be an indicator for a reduced accessibility for microorganisms during anaerobic digestion.<sup>[37]</sup>

### 3.1.4. Cellulose Crystallinity

**Figure 4a** exemplarily shows FTIR spectra recorded for test series conducted with the same residence time at different temperatures in comparison with untreated reed. In **Figure 4b**, the calculated cellulose CI is shown for all samples. According to the results presented in Section 3.1.2, cellulose is considered the main component that can be degraded anaerobically. Chemically speaking, cellulose is a linear polymer consisting of D-glucose subunits interconnected by β-1,4-glycosidic linkages. Within lignocellulosic biomass, it is present in the form of microfibrils, which have both crystalline and amorphous regions, whereby amorphous cellulose is easier to hydrolyze.<sup>[38]</sup> A higher amount of amorphous cellulose could therefore be beneficial for anaerobic digestion. The displayed FTIR spectra show only minor differences. Mainly, the height of the absorption peaks changes, which indicates an increasing disruption of the lignocellulosic structure with increase in treatment temperature. Regarding the calculated CI, vapothermal pretreatment at temperatures ≤ 150 °C does not significantly change the type of cellulose present in the samples. However, at higher temperatures, the CI increases, indicating a larger part of crystalline cellulose. In this regard it has to be noted that changes in CI might not only be a consequence of reduced amorphous cellulose but can also be attributed to recrystallization of amorphous cellulose after vapothermal pretreatment. Such an effect was already observed for several thermal treatment methods such as torrefaction<sup>[39]</sup> and steam explosion.<sup>[40]</sup> Most likely, this can be traced back to removal of hemicellulose and recrystallization of amorphous cellulose at such high temperatures. A possible expected additional yield of biogas after anaerobic digestion due

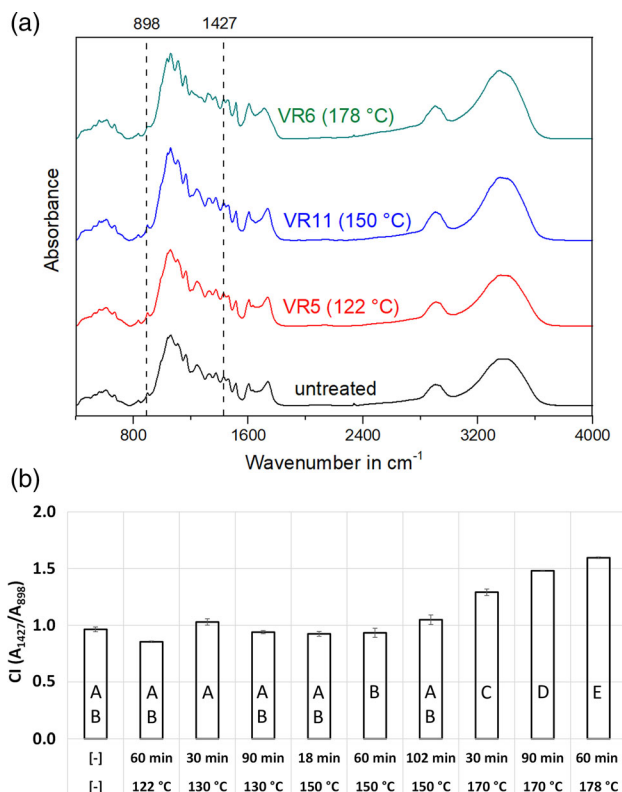


**Figure 4.** a) FTIR spectra for selected test series with 60 min residence time and b) respective CI values for all samples—different letters indicate significant differences between mean values according to the Tukey–Kramer test ( $\alpha = 0.05$ ).

to structure disruption and the associated higher accessibility for microorganisms could be cancelled out by the higher cellulose crystallinity. The findings in this study are contrary to the findings for hydrothermal pretreatment, where a decrease in CI after pretreatment was recorded for sunflower stalks and safflower straw<sup>[35,41]</sup> but was in accordance to the findings for the more related process of steam explosion. For steam-exploded wheat straw, higher biogas yields were reported after treatment at 180 °C, although an increase in crystallinity occurred,<sup>[27]</sup> which denotes that in the considered case, the increased accessibility for microorganisms outweighed the negative effects of increased crystallinity.

## 3.2. Effects of Vapothermal Pretreatment on Anaerobic Digestibility

In the following, results of the batch fermentation tests are presented and discussed. First, the influence of vapothermal pretreatment on total biogas and methane yield is presented. Then, a closer look on degradation velocity is taken.

### 3.2.1. Biogas and Methane Yield

Biogas and methane yields of untreated as well as vapothermal pretreated reed samples are shown in **Figure 5**. The test series at 150 °C and residence time of 18 min are not included due to analytical errors. During biogas production tests, no inhibition

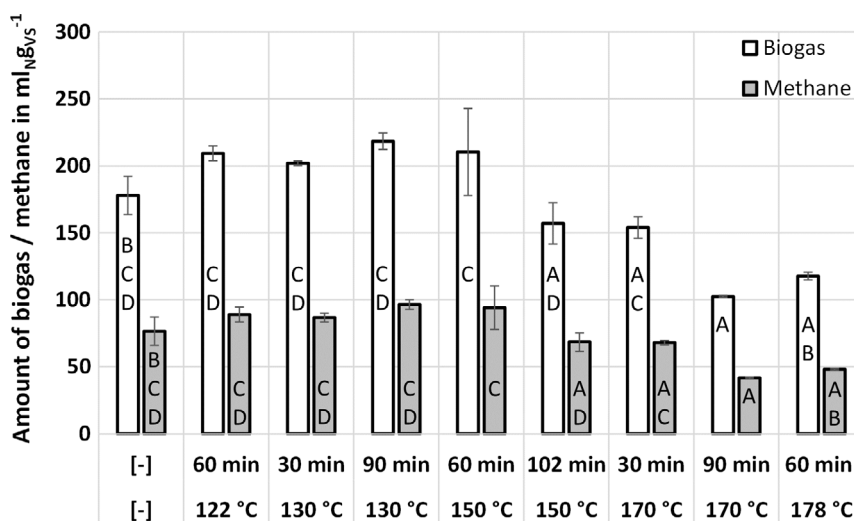


**Figure 5.** Biogas and methane yields before and after vapo-thermal pretreatment—different letters indicate significant differences between mean values according to the Tukey–Kramer test ( $\alpha = 0.05$ ).

was detected in any of the test series. Furthermore, there were only slight differences in the methane yield. The mean value of the measured methane contents was  $44 \pm 2\%$ . Highest biogas and methane yields of  $218.4 \pm 6.2$  and  $96.5 \pm 3.5$  mL<sub>NgVS</sub><sup>-1</sup> were found for reeds pretreated at 130 °C for 90 min, respectively. This equals an increase in biogas and methane yield of 23% and 26% compared with the untreated sample, respectively. However, according to the Tukey–Kramer test ( $\alpha = 0.05$ ), this increase was not statistically significant. A trend of increasing biogas and methane yields can be identified for samples pretreated at temperatures  $\leq 150$  °C. However, this trend is already reversed at 150 °C, when long residence times are used (i.e., 102 min). At higher treatment temperatures, this negative trend continues. Lowest amounts of  $102.5 \pm 0.7$  and  $41.7 \pm 0.7$  mL<sub>NgVS</sub><sup>-1</sup> for biogas and methane yield were found after treatment at 170 °C and 90 min, respectively. Compared with the untreated sample, this equals a decrease of 42 and 37%, respectively. In this case, the decrease was statistically significant. Reduction in both biogas and methane yield can be explained by the relatively increased share of lignin (Section 3.1.2) and decreased substrate accessibility for microorganisms indicated by reduced WHC (Section 3.1.3). Furthermore, increase in cellulose crystallinity (Section 3.1.4) further promotes this decrease. Results in this study differ from results of similar pretreatment techniques such as steam explosion, where an increase in biogas and methane yields up to treatment temperatures of 220 °C.<sup>[19]</sup> This could be traced back to a more severe reaction of simple sugars released from the biomass matrix during vapo-thermal pretreatment due to comparatively longer residence times. The resulting reaction products such as phenolic compounds and furan derivatives are known to inhibit anaerobic digestion.<sup>[23]</sup> Differences in biomass composition could also be responsible for a different behavior during thermal pretreatment. In this study, the parameters were varied in a relatively wide range, as no findings on the optimum conditions of vapo-thermal pretreatment for enhancement of anaerobic digestibility of reeds are available so far. From the results presented here, it becomes clear that the optimum

conditions are at temperatures  $\leq 150$  °C. Further investigations in the range between 130 and 150 °C are recommended to investigate how far total biogas and methane yield can be increased by vapo-thermal pretreatment. In these investigations, it should also be investigated as to what extent inhibiting substances are already formed at this relatively low temperature level. From the literature, it is known that during thermal degradation of various sugars, e.g., hydroxymethylfurfural and furfural can be formed.<sup>[42,43]</sup> The decomposition of lignin could, e.g., lead to the formation of phenol, whereas during decomposition of proteins, so-called melanoidins can be formed. Further Maillard products could arise from reactions between carbohydrates and proteins.<sup>[44]</sup> In sufficiently high concentrations, all these reaction products can inhibit anaerobic degradation. However, due to the earlier described temperature ranges in which the cell wall components are decomposed (see Section 3.1.1), it is unlikely that such high concentrations of inhibitors are formed at temperatures  $\leq 150$  °C. This assumption is supported by various studies in which tests were conducted for hydrothermal pretreatment of lignocellulosic biomass with only little formation of inhibiting substances that did not harm the anaerobic degradation process (e.g., see various studies<sup>[35,45]</sup>).

Both biogas and methane yields obtained are relatively low when compared with literature results, where biogas yields of around 300 mL<sub>NgVS</sub><sup>-1</sup> are reported.<sup>[19]</sup> A possible reason therefore is the long life of the plants before the harvest (plants were harvested after 8 years without previous pruning) and the relatively hot climate at the sampling location, which both promote lignification.<sup>[46]</sup>

### 3.2.2. Degradation Velocity

**Figure 6** shows the ratio of biogas formation after 7 days and total biogas formation after 32 days ( $R7/32$ ) for both untreated and pretreated reed samples. This representation was chosen to evaluate changes in degradation velocity. Accelerated degradation

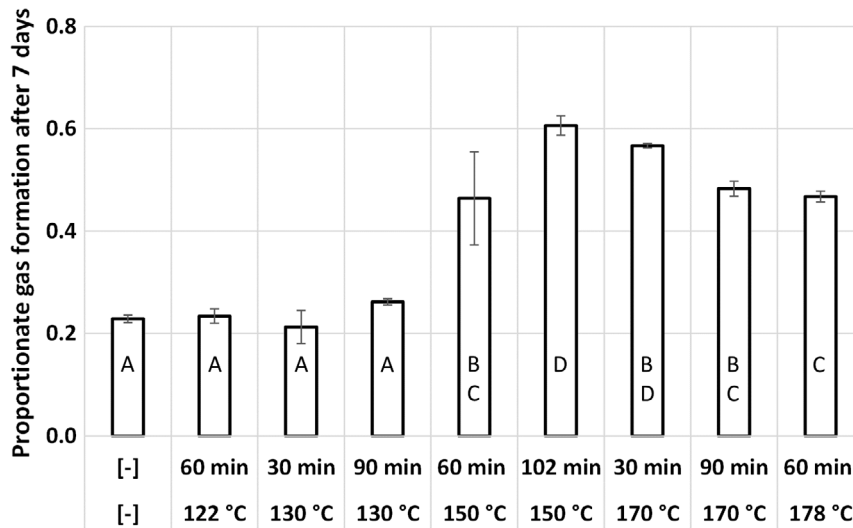


**Figure 6.** Ratio of biogas formation after 7 days and total biogas formation after 32 days—different letters indicate significant differences between mean values according to the Tukey–Kramer test ( $\alpha = 0.05$ ).

velocity can have a positive effect on the total costs of a biogas plant, as the residence time for anaerobic digestion can be decreased and thus more substrate can be fermented per time. However, care must be taken to ensure that the residence time is long enough so that no more microorganisms are washed out of the system than are formed simultaneously. At temperatures  $\leq 130\text{ °C}$ , pretreatment had no significant effect on  $R_{7/32}$ , but pretreatment at  $\geq 150\text{ °C}$  significantly enhanced this ratio. The highest value of  $0.61 \pm 0.02$  was found for reeds pretreated at  $150\text{ °C}$  for 102 min. This means that vapothermal pretreatment

at these conditions was able to almost triple biogas formation within the first 7 days of anaerobic digestion. This increase could have different reasons. On the one hand, degradable components might be more easily accessible for microorganisms due to a partial breakdown of the biomass matrix. On the other hand, the rate-determining phase of hydrolysis could have been accelerated due to the presence of more easily degradable substances such as monosaccharides released during vapothermal pretreatment. Furthermore, fatty acids produced during vapothermal pretreatment can be directly converted into biogas. At more severe

**Table 3.** Kinetic parameters of the determined models.

Test series	Model	$P$ [ $\text{mL}_N \text{ gVS}^{-1}$ ]	$R_m$ [ $\text{mL}_N \text{ gVS}^{-1} \text{ d}^{-1}$ ]	$\lambda$ [d]	$R^2$ [-]	RMSE [ $\text{mL}_N \text{ gVS}^{-1}$ ]
Untreated	Gompertz	177.4	8.8	2.4	0.999	1.60
	Transference	244.1	10.0	1.2	0.986	6.74
122 °C 60 min	Gompertz	240.5	8.3	1.2	0.998	3.14
	Transference	447.9	8.9	0.3	0.995	4.53
130 °C 30 min	Gompertz	223.8	8.7	2.1	0.999	2.39
	Transference	389.1	9.3	0.9	0.993	5.46
130 °C 90 min	Gompertz	232.9	9.8	0.9	0.998	3.29
	Transference	320.7	11.9	0.5	0.994	5.36
150 °C 60 min	Gompertz	206.3	11.0	-2.4	0.980	7.79
	Transference	218.5	19.0	-0.7	0.994	4.23
150 °C 102 min	Gompertz	150.0	10.9	-2.1	0.967	6.68
	Transference	153.9	20.3	-0.6	0.989	4.17
170 °C 30 min	Gompertz	149.6	10.5	-1.9	0.981	5.40
	Transference	154.2	18.9	-0.5	0.993	3.42
170 °C 90 min	Gompertz	101.1	5.9	-1.8	0.986	3.20
	Transference	106.7	10.0	-0.5	0.993	2.37
178 °C 60 min	Gompertz	115.5	6.4	-1.8	0.987	3.67
	Transference	123.0	10.8	-0.5	0.996	2.07

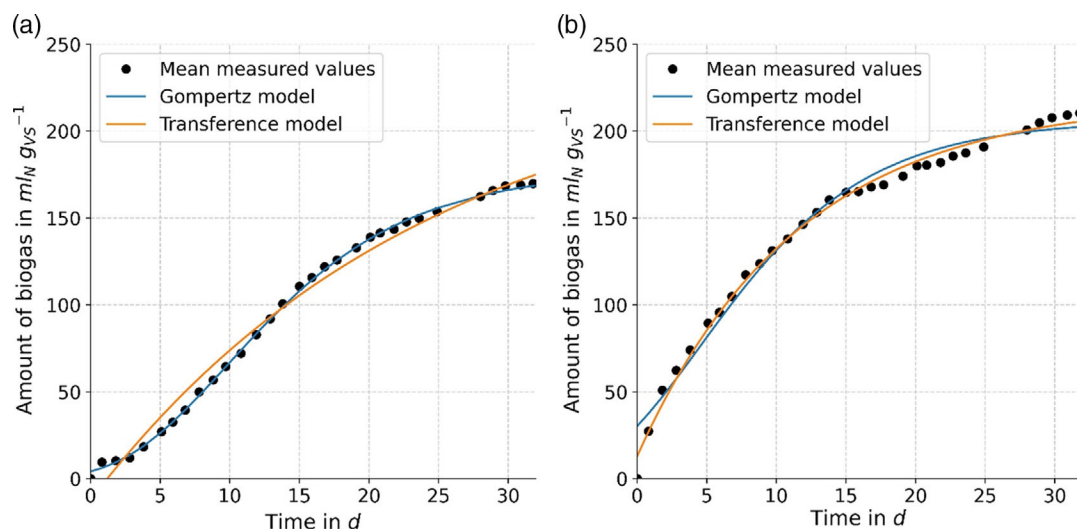


**Figure 7.** Cumulative biogas production—experimental and model data for a) untreated reed and b) vapothermal pretreated reed at 150 °C and 60 min.

pretreatment conditions,  $R7/32$  declines again but remains above the level of untreated reeds. Most likely, the initially accelerated hydrolysis and conversion of short-chain fatty acids, which presumably are derived from the decomposition of hemicellulose during vapothermal pretreatment, are followed by decelerated further anaerobic degradation due to the same reasons responsible for a lower overall gas yield (Section 3.2.1). These findings are to a large part in accordance with findings for steam explosion pretreatment, for which also reduction in initial lag phase and faster overall anaerobic decomposition were reported.<sup>[27,47]</sup>

The estimated kinetic parameters for both model types and their respective  $R^2$  and RMSE values are shown in **Table 3**.

The results obtained with  $R7/32$  could also be confirmed by the developed kinetic models. The kinetic parameter  $\lambda$ , which indicates the duration of the initial lag phase during biogas production, has negative values for the pretreatment conditions that also lead to comparable high  $R7/32$  ratios in both types of model. This means that at these conditions, vapothermal pretreatment significantly reduces lag phase during subsequent anaerobic digestion. This is exemplarily shown in **Figure 7** for the biogas formation of untreated reeds compared with reeds after vapothermal pretreatment at 150 °C for 60 min. The  $R^2$  values, which are all relatively close to 1, as well as the relatively low RSME values, show that the determined models match the measured data relatively well. However, the transference models significantly overestimate the biogas formation potential for vapothermal pretreatment below 150 °C. As the models have not been further verified to date, the prediction of total biogas yields from them is quite uncertain and the models should only be used for the studied period of 32 days.

#### 4. Conclusion

The aim of this study was to investigate the effect of a vapothermal pretreatment on the anaerobic digestibility of reeds. Both temperature and residence time during pretreatment were varied. The responsible effects of changes in digestibility should

be identified with the help of accompanying analytics regarding structure and composition of the biomass. Therefore, among others, the cell wall composition, particle size distribution, WHC, and cellulose crystallinity were determined. The main findings are as follows. 1) Vapothermal pretreatment can significantly improve degradation velocity during anaerobic digestion but, under the pretreatment conditions chosen in this study, was not able to significantly improve total biogas/methane yield. 2) Various positive effects on anaerobic digestibility such as improvement of grindability and pore volume as well as a partial breakdown of the biomass matrix were identified for vapothermal pretreatment of reeds. 3) At severe reaction conditions of pretreatment, the positive effects were reversed. Inter alia, possible reasons therefore can be an increase in both cellulose crystallinity and share of lignin, as well as the formation of inhibiting substances. 4) The optimum conditions for vapothermal pretreatment of reeds seem to be in a temperature range between 130 °C and 150 °C. Further attempts to optimize the pretreatment conditions should be conducted.

#### Acknowledgements

Open access funding enabled and organized by Projekt DEAL.

#### Conflict of Interest

The authors declare no conflict of interest.

#### Data Availability Statement

Research data are not shared.

#### Keywords

anaerobic digestion, biogas, common reeds, vapothermal pretreatments

Received: December 1, 2020  
Revised: April 1, 2021  
Published online: May 4, 2021

- [1] Bayerische Landesanstalt für Umwelt, *Biogashandbuch Bayern – Materialband: Kapitel 1.1–1.5, Augsburg 2007*.
- [2] Fachverband Biogas, *Biogas Market Data in Germany 2018/2019*, Fachverband Biogas e.V., Freising **2019**.
- [3] T. Nevzorova, V. Kutcherov, *Energy Strategy Rev.* **2019**, 26, 100414.
- [4] *Renewable Energy Sources: Engineering, Technology, Innovation: ICORES 2017. Springer Proceedings in Energy* (Ed.: K. S. Mudryk), Springer, Cham **2018**.
- [5] J. F. Köbbing, N. Thevs, S. Zerbe, *Mires Peat* **2013**, 13, 1.
- [6] P.-A. Hansson, H. Fredriksson, *Agric. Ecosyst. Environ.* **2004**, 102, 365.
- [7] T. T. Allen, *Introduction to Engineering Statistics and Lean Six Sigma: Statistical Quality Control and Design of Experiments and Systems*, 3rd ed, Springer, London **2019**.
- [8] J. Dufner, U. Jensen, E. Schumacher, *Statistik mit SAS*, 3rd edn, Teubner Verlag, Wiesbaden **2004**.
- [9] *DIN EN 15935: Sludge, treated biowaste, soil and waste – Determination of loss on ignition:1–12*, **2020**, <https://doi.org/10.31030/3134550>.
- [10] *DIN EN 15933: Sludge, treated biowaste and soil – Determination of pH:1–12*, **2012**, <https://doi.org/10.31030/1866552>.
- [11] VDLUFA, *The chemical analysis of feedstuffs*, 8th edn, VDLUFA-Verlag, Darmstadt **2012**.
- [12] *DIN 51938: Testing of carbonaceous materials – Determination of particle size distribution by sieving – Solid matters:1–8*, **2015**, <https://doi.org/10.31030/2327673>.
- [13] H. Günzler, H.-U. Gremlich, *IR-Spektroskopie: Eine Einführung*, 4., vollständig überarbeitete und aktualisierte Aufl., Wiley/Wiley-VCH, Hoboken, NJ/Weinheim **2003**.
- [14] F. G. Hurtubise, H. Krassig, *Analyt. Chem.* **1960**, 32, 177.
- [15] M. L. Nelson, R. T. O'Connor, *J. Appl. Polym. Sci.* **1964**, 8, 1311.
- [16] K. Karimi, M. J. Taherzadeh, *Bioresour. Technol.* **2016**, 200, 1008.
- [17] *VDI 4630: Fermentation of organic materials: Characterisation of the substrate, sampling, collection of material data, fermentation tests: 1–132*, **2016**.
- [18] L. Li, X. Kong, F. Yang, D. Li, Z. Yuan, Y. Sun, *Appl. Biochem. Biotechnol.* **2012**, 166, 1183.
- [19] J. Lizasoain, M. Rincón, F. Theuretzbacher, R. Enguídanos, P. J. Nielsen, A. Potthast, T. Zweckmair, A. Gronauer, A. Bauer, *Biomass Bioenergy* **2016**, 95, 84.
- [20] G. Fuchs, H. G. Schlegel, T. Eitinger, *Allgemeine Mikrobiologie: 53 Tabellen*, 8., vollst. überarb. und erw., Aufl. Thieme, Stuttgart **2007**.
- [21] X. Luo, J.Y. Zhu, *Enzyme Microb. Technol.* **2011**, 48, 92.
- [22] M. Scherzinger, M. Kaltschmitt, *Renew. Sustain. Energy Rev.* **2021**, 137, 110627.
- [23] A. Bauer, J. Lizasoain, F. Theuretzbacher, J. W. Agger, M. Rincón, S. Menardo, M. K. Saylor, R. Enguídanos, P. J. Nielsen, A. Potthast, T. Zweckmair, A. Gronauer, S. J. Horn, *Bioresour. Technol.* **2014**, 166, 403.
- [24] S. Nizamuddin, H. A. Baloch, G.J. Griffin, N.M. Mubarak, A. W. Bhutto, R. Abro, S. A. Mazari, B. S. Ali, *Renew. Sustain. Energy Rev.* **2017**, 73, 1289.
- [25] L. He, H. Huang, Z. Zhang, Z. Lei, *Curr. Org. Chem.* **2015**, 19, 437.
- [26] L. Leible, S. Kälber, G. O. Kappler, H. Oechsner, M. Mönch-Tegeder, *Biogas aus Landschaftspflegegras: Möglichkeiten und Grenzen*, KIT Scientific Reports, Vol. 7691, Technische Informationsbibliothek u., Universitätsbibliothek/KIT Scientific Publishing, Hannover/Karlsruhe **2015**.
- [27] A. A. Rajput, A. A. Zeshan, C. Visvanathan, *J. Environ. Manage.* **2018**, 221, 45.
- [28] S. Menardo, G. Airoidi, P. Balsari, *Bioresour. Technol.* **2012**, 104, 708.
- [29] A. Mshandete, L. Björnsson, A. K. Kivaisi, M.S.T. Rubindamayugi, B. Mattiasson, *Renew. Energy* **2006**, 31, 2385.
- [30] L. Wang, E. Barta-Rajnai, Ø. Skreiberg, R. Khalil, Z. Czégény, E. Jakab, Z. Barta, M. Grønli, *Appl. Energy* **2018**, 227, 137.
- [31] M. Scherzinger, T. Kulbeik, M. Kaltschmitt, *Fuel* **2020**, 273.
- [32] M. J. Prins, K. J. Ptasiński, F. J. Janssen, *Energy* **2006**, 31, 3458.
- [33] L. Kratky, T. Jirout, *Chem. Eng. Technol.* **2011**, 34, 391.
- [34] B. Arias, C. Pevida, J. Feroso, M.G. Plaza, F. Rubiera, J.J. Pis, *Fuel Process. Technol.* **2008**, 89, 169.
- [35] S. S. Hashemi, K. Karimi, S. Mirmohamadsadeghi, *Energy* **2019**, 172, 545.
- [36] A. Kongdee, T. Bechtold, E. Burtscher, M. Scheinecker, *Carbohydrate Polym.* **2004**, 57, 39.
- [37] J. Zhao, H. Chen, *Chem. Eng. Sci.* **2013**, 104, 1036.
- [38] S. Malherbe, T.E. Cloete, *Rev. Environ. Sci. Biotechnol.* **2002**, 1, 105.
- [39] J.-L. Wen, S.-L. Sun, T.-Q. Yuan, F. Xu, R.-C. Sun, *Appl. Energy* **2014**, 121, 1.
- [40] A. Lorenzo-Hernando, J. Martín-Juárez, S. Bolado-Rodríguez, *Carbohydrate Polym.* **2018**, 191, 234.
- [41] S. M. Hesami, H. Zilouei, K. Karimi, A. Asadinezhad, *Ind. Crops Prod.* **2015**, 76, 449.
- [42] D. Kim, *Molecules* **2018**, 23, 309.
- [43] T. Miyazawa, S. Ohtsu, T. Funazukuri, *J. Mater. Sci.* **2008**, 43, 2447.
- [44] Y. Fan, U. Hornung, N. Dahmen, A. Kruse, *Biomass Conv. Bioref.* **2018**, 8, 909.
- [45] L. M. López González, I. Pereda Reyes, J. Dewulf, J. Budde, M. Heiermann, H. Vervaeren, *Bioresour. Technol.* **2014**, 169, 284.
- [46] F. Dragoni, V. Giannini, G. Ragolini, E. Bonari, N. Silvestri, *Bioenergy Res.* **2017**, 10, 1066.
- [47] V. Vivekanand, E. F. Olsen, V. G. Eijsink, S. J. Horn, *Bioresour. Technol.* **2013**, 127, 343.